System Level Simulation of Mixed-signal Multi-domain Microsystems with Piecewise Linear Behavioral Models[1]

José A. Martínez[α], Timothy P. Kurzweg[β], Steven P. Levitan[α], Abhijit J. Davare[γ], Michael Bails[α], Mark Kahrs[α], Donald M. Chiarulli[δ]

[α]University of Pittsburgh, EE Department, Pittsburgh, PA USA 15261
[β]Drexel University, ECE Department, Philadelphia, PA USA 19104
[γ]University of California at Berkeley, EECS Department, Berkeley, CA USA 94720
[δ]University of Pittsburgh, CS Department, Pittsburgh, PA USA 15260

ABSTRACT

In this paper, we present a component-based multi-level mixed-signal design and simulation methodology that provides a solution to the problem of accurate modeling and simulation of mixed signal, multi-domain (MSMD) systems. This is achieved by first, partitioning the system into components that are modeled by analytic expressions at the behavioral level; and second, integrating these expressions into component behavioral solvers using a combination of piecewise linear (PWL) modeling and Modified Nodal Analysis (MNA). At the system level, a discrete event simulator sends composite signals between these components and manages multiple timescales and feedback. Simulation speed and accuracy can be tuned by controlling the granularity of the regions of operation of the devices, the sample density of optical wavefronts, and the time resolution of the discrete event simulator. The methodology is specifically optimized for loosely coupled systems of complex components such as the ones found in multi-domain microsystems.

Keywords: System level simulation, behavioral modeling, piecewise linear simulation, Modified Nodal Analysis, MEMs simulation.

1 INTRODUCTION: SYSTEM LEVEL SIMULATION

The simulation of multi-domain systems is challenging since it is based on signals with different properties (e.g., voltage for electronics, force for mechanics and intensity for optics) and with varied dynamics. We address this problem with a multi-level simulation environment.

At the highest level, the system can be considered as being composed of component modules that are individually characterized and joined together by the mutual exchange of information. In Figure 1(a), this representation of a general dynamic system is shown. Each module, *i*, processes some vector of input messages, $X_i(t)$, updates its vector of internal state variables, $S_i(t)$, and generates sets of output messages[1]. The dynamics in this representation can be modeled using a discrete event (DE) computation model where each module's execution is based on the availability of new data values for its inputs. Under this scheme, differences in data rates on multiple input streams for components are controlled by making use of buffering.

The components are modeled at the behavioral level where they are represented either by analytic expressions or as a tightly coupled network of elements such as shown in Figure 1(b). In either case, at the system level, there is a loosely coupled network of tightly coupled component models. This corresponds well with the general structure of mixed-signal microsystems where multi-domain components interact with few signals, while at the same time; the behavior of each component is based on its underlying physical processes.

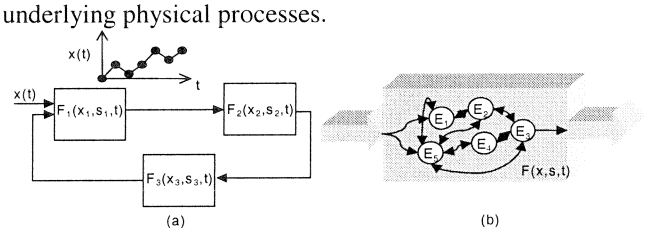

Figure 1: System modeling methodology (a)Inter-component; and (b) Intra-component interactions

1.1 Behavioral Modeling Methodology

As shown in Figure 1(b), each component can be described as a network of linear and non-linear elements with ports defined as pairs of nodes between the elements.

In previous work [2], we introduced our combined piecewise linear (PWL) and Modified Nodal Analysis (MNA) representation for the simulation of multidomain components at the system level. The use of a PWL general solver decreases the computational task and allows for a trade-off between accuracy and speed. In this paper, we focus on the automatic generation of linear templates for non-linear devices as used in our methodology.

1.2 Piecewise Linear Model Generation

The nodal analysis principle can be traced back to the basic conservation laws of energy and bond graph theory [1]. In an enclosed volume with finite interfaces, an energy conservation relationship can be established using the

[1] This work was supported in part by DARPA, under Grant No. F49620-01-1-0536 and NSF, under Grant No. C-CR9988319

energy flow through the interfaces and the internal energy density. These volumes can then be characterized as "nodes" where this conservation law holds. The behavior of each element is captured in terms of the analytic relationships among variables, which define the state of its nodes. The two basic types of variables in nodal analysis are *across* and *through* variables. Across variables are measures of the values of field potential in the physics of the device (e.g., electrical potential, temperature, fluid pressure). Through variables are measures of flux intensity at nodes (e.g., electrical current, thermal flux, fluid velocity).

Consequently, for any element in the nodal representation a function f can be found that relates the total flows (across variables) through its interfaces (nodes) as equal to zero.

If we define the state of the element $\hat{s}(t)$ as being a vector of all its across variables $\hat{x}_{cr}(t)$, through variables $\hat{x}_{th}(t)$ and their associated (n) derivatives for all its m nodes at time t then the nodal function f is defined as: $f(\hat{s}) = 0;$

where $\hat{s} = [(\hat{x}_{cr}, \hat{x}_{cr}^{'}, \hat{x}_{cr}^{''}, ...\hat{x}_{cr}^{(n)}),.(x_{th}, x_{th}^{'}, \hat{x}_{cr}^{''}, ...\hat{x}_{cr}^{(n)})]^T$. The linearization of this function can be obtained through a Taylor expansion around a point $\hat{s}_c$ where the function is differentiable.

$$f(\hat{s}) \cong f(\hat{s}_c) + f(\hat{s}_c)'(\hat{s} - \hat{s}_c) \cong 0 \quad (1)$$

Equation (1) is a set of Ordinary Differential Equations (ODE) of order n, in a vector form, that represents the piecewise linear equivalent of the device at time t. Additionally, this expression is in a nodal form that can be mapped directly to a MNA formulation. The relevance of this formulation is that it can include both multi-domain variables as well as non-linear elements. The additional complexity of order n for the ODE can be resolved using an appropriate variable change that reduces the expression to first order.

To expand this linearization further than a point on the domain of the function, we divide the domain hyperspace into regions where a hyperplane can be closely matched to $f(\hat{s})$. This gives us the ability to approximate the function to the degree of accuracy required for the range of operation of interest. This linear approximation of $f_i(\hat{s})$ is done for each of the i ($1 < i < m$) nodes that make up the ports of the element.

We use a triangulation approach, as shown in Figure 2, based on recursive decomposition of the function domain hyperspace into hypercubic regions of operation followed by a vertex index permutation approach for triangulation into hyperlinear regions of operation.

Figures 2(a) and (b) illustrate the case for three dimensions. After recursive decomposition of the space into cubes, each cube (in Figure 2(a)) represents an interval on the domain for a function of three variables ($F(u_1,u_2,u_3)$). In Figure 2(b), we show the tetrahedral triangulation of a single 3D cube, where each tetrahedron is a linear approximation of the function. As an example of this method, in Figure 3(a) we show the 2D linearization of the NMOS transistor I_{ds} equation to %1 relative accuracy.

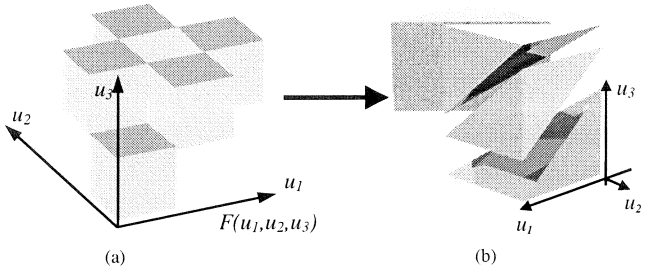

Figure 2: a) Function $F(u_1,u_2,u_3)$ decomposed into hypercubes b) Decomposition of cube into six tetrahedrons

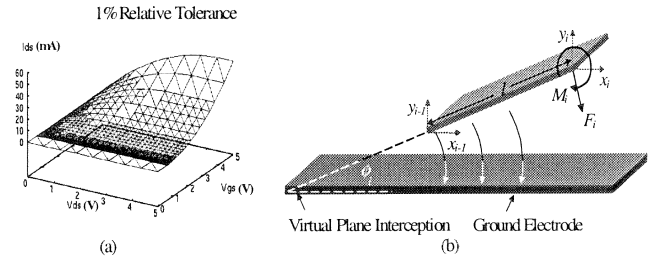

Figure 3: (a) 2D Linearization of NMOS transistor, I_{ds} vs. V_{gs} and V_{ds} for 1% relative accuracy (b) Electrostatic modeling on a single elemental beam

1.3 Multi-domain simulation

As an example of the integration of different domains into an MNA-PWL simulation, we next describe the modeling of electrostatic effects on a mechanical structure.

For the electrostatic modeling of forces we consider a single elemental beam as shown in Figure 3(b). The surface defined by this single flat basic element intercepts the substrate plane in a line that can be considered a virtual axis for the relative coordinate system. This element is considered a part of a "structural ensemble" which makes up a complete structure. The modeling is based on considering the sub-structure as an inclined flat capacitor. The distributed electrostatic forces are analytically represented as concentrated forces applied over the last node of the basic beam. The electrostatic force over the element i is given by:

$$F_i = \left(\frac{\varepsilon w V^2}{l} \right) \frac{(y_i - y_{i-1})^2}{\phi_i^2 y_i y_{i-1}} \quad (2)$$

In this expression, the ϕ represents the angle between both planes, V is the applied voltage, l is the length of the elemental beam, w is the width of that element, y_i and y_{i-1} are the y coordinates of the nodes in the global reference system, and ε is the electric permitivity of the medium between the plates.

The electrostatic torque over the element i is given by:

$$M_i = F_i \frac{\Delta x_i}{l} x_{i-1} + F_i \frac{\Delta x_i}{l} \frac{\Delta x_i}{\Delta y_i} y_{i-1} \left(\frac{y_i}{\Delta y_i} \ln\left(\frac{y_i}{y_{i-1}} \right) - 1 \right) + F_i \frac{y_i}{l} y_{i-1} \ln\left(\frac{y_i}{y_{i-1}} \right) \quad (3)$$

These analytical expressions describe the electrostatic behavior for the basic element. Using a PWL linearization technique as the one described above these expressions are reduced to a PWL model of the form:

$$F_i = A_i V + A_i y_i + A_{i-1} y_{i-1} + A_0;$$
$$M_i = B_i V + B_i y_i + B_{i-1} y_{i-1} + C_i x_i + C_{i-1} x_{i-1} + B_0 \quad (4)$$

These expressions are linear templates that capture the non-linear behavior of equations (2) and (3) through a set of regions of operations each one with a corresponding set of coefficients $(A_i,....A_0), (B_i,....B_0), (C_i,....C_0)$. These models can then be integrated to the representation of the structural ensemble.

As can be seen, for this model there is no distinction between variables from either the mechanical or the electrical domains. The direct relationship between the domains is the key for this multi-domain model. In fact it is these relationships that embody the behavior of the electrostatic transducer and govern the conversion of energy between domains.

2 EXAMPLE SYSTEM: A GRATING LIGHT VALVE (GLV) PROJECTOR

To illustrate the capabilities of our mixed-signal, multi-domain methodology, we examine one of the more promising optical Micro-Electro-Mechanical (MEM) components, the Grating Light Valve (GLV) [3]. This device has many display applications, including digital projection, HDTV, and vehicle displays. The GLV is simply a MEM phase grating made from parallel rows of reflective ribbons. Figure 4 shows the ribbons, from both a top and side view, and also the optical reflection patterns during the operation of the device. When all the ribbons are in the same plane, incident light that strikes normal to the surface reflects 180 degrees off the GLV creating the so called 0^{th} mode of a diffraction pattern, as shown in Figure 4(b). However, if alternating ribbons are moved down a quarter of a wavelength (λ/4) of the incident optical light, a "square-well" diffraction pattern is created, and the light is reflected at an angle from that of the incident light, into the odd ($\pm 1^{st}$) diffractive modes, as shown in Figure 4(c). The angle of reflection depends on the width of the ribbons and the wavelength of the incident light.

For the simulations of the GLV, we examine one optical pixel. A projected pixel is diffracted from a GLV composed of 4 ribbons, two stationary and two that are movable. Each ribbon has a length of $60\mu m$, a width of $5\mu m$, and a thickness of $1.5\mu m$, for a total GLV pixel size of $60x20\mu m$. The ribbons are made of silicon nitrite (density 3290 Kg/m^3, Young's modulus 290x10^9 N/m^2), and coated with aluminum for smoothness and reflectivity.

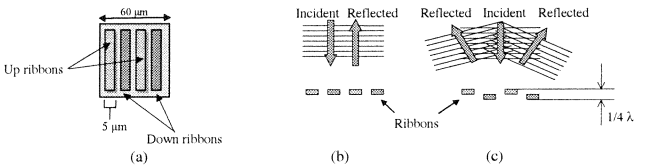

Figure 4: GLV Device (a) Top View; and Side View Operation for (b) Up Ribbons and (c) Down Ribbons

Each ribbon moves through electro-static attraction between the ribbon and an electrode fabricated underneath the ribbon. Therefore, the model of the GLV is two fold: an electro-mechanical model simulating the movement of the ribbons towards the substrate, and the optical model, simulating the reflection of the optical wavefront off of the ribbons.

The ribbon is modeled as a thin beam anchored on each end sitting 650nm above a silicon substrate, which is covered with 500 nm of oxide. The ribbon is modeled with the techniques presented earlier. The voltage is applied between the ribbon and substrate electrode by a 2-stage CMOS amplifier.

Since the ribbon ends are anchored, the alternating ribbons bend as they are pulled to the substrate. In the simulations, the ribbon is composed of an equal sized number, *N,* of segments or beams, totaling *N+1* nodes. The layered shape of the ribbon with forces and movement limited to one plane justify the use of the basic beam element for the modeling of the mechanical structure with the analysis reduced to a two-dimensional problem in the plane of the displacement.

2.1 Diffractive Optical simulation

For the optical simulation, our angular spectrum technique is used for a fast diffractive optical propagation solution, based on gridded scalar wavefront messages in the Fourier domain [4]. The effect of the ribbon movement is optically modeled as a phase grating, where the light that strikes the "down" ribbons propagates further than the light that strikes the "up" ribbons. Light reflecting from the down ribbons is multiplied by a phase term, which is similar to a propagation term through a medium: $U_{down\_ribbon} = U \exp(j2kd)$, where, d is the distance that the ribbon is moved towards the substrate and k is the wave number, $k = 2\pi / \lambda$.

For this example, we simulate optical propagation with both ideal flat ribbons and realistic curved ribbons. Figure 5 compares three cases. Figure 5(a) shows no ribbon movement and reflection in the 0^{th} mode; 5(b) shows the 1^{st} order diffraction from alternating ideal flat ribbons being pulled down a distance of λ/4, and 5(c) diffraction from a curved ribbon where the optical intensity contour is a combination of 0^{th} and 1^{st} order modes. Even for the curved ribbon, we can see, as the ribbons are attracted to the substrate, more optical power is diffracted into the non-zero modes. This is the light that is used for the projection of the desired image.

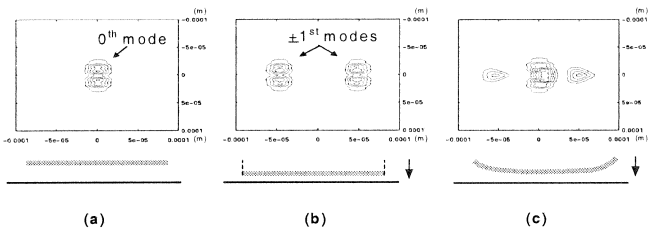

Figure 5: GLV Operation (a) Ribbons all up (b) Ideal Displacement (c) Curved Ribbon Displacement

2.2 System-Level Simulation Performance

The accuracy of the mechanical simulation was compared to modal analysis of the ribbon using ANSYS. An 11-node model matches the nine first modal frequencies with a maximum difference of 2.24 % at the highest frequency; while, for a 21-node model the 10^{th} modal frequency differs by less than 0.59 %. A 41-node model reduces this difference to 0.15%. As expected, to accurately capture higher modal frequencies, a larger discretization is required.

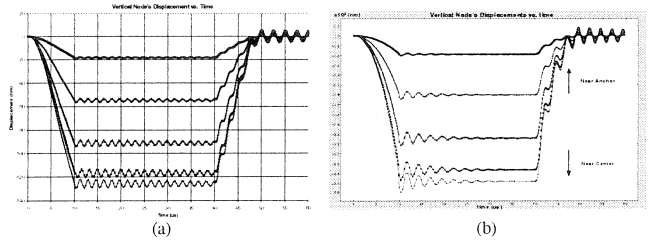

Figure 6: Nodal displacements in 11-node ribbon model with high frequency drive signal (10 μs switching time) (a) ANSYS (b) Chatoyant

Figure 6 shows the dynamic response of the ribbon driven at a high switching frequency. The high stiffness of the structure gives it a fast response time as observed. However, under this stimulus, resonant effects are observed in the displacement of the nodes. The visible pattern of damped oscillations shows that the stiffness affects the maximum operating speed of this device.

The damping of MEM structures in a laminar fluid is a very difficult problem. In ANSYS, this is characterized as ideal spring damping elements to avoid the costly computation of a complete fluid analysis using the Navier-Stokes formulation; the result is shown in Figure 6(a). In our methodology we chose to include the effect directly in the damping matrix of the structure, which allows the damping to affect displacement in every degree of freedom of the element; the result is shown in Figure 6(b). However, we are still using a typical constant value for this effect. A more rigorous damping analysis considering the non-linear laminar fluidic effect over the structure is required for both techniques and it is currently under development.

Table 1 shows system simulation time in seconds[2] as a function of both the optical scalar mesh resolution and the number of segments in the ribbon. The mechanical subsystem time includes the initialization of the MNA as well as the solution times for the entire movement for the 2.4ms stimulus. The optical subsystem time includes both the scalar propagation time and the detector power integration time. The system time includes the electrical simulation of the CMOS driver, as well as initialization overhead.

What is interesting to note is the range of simulation time, from 3 seconds for the 5-element, 128x128 case to 168 seconds for the 41-element, 512x512 case, which corresponds to an increase in fidelity of the resulting optical waveforms and mechanical characterizations achieved.

What this illustrates is that we can use the same behavioral descriptions, in the same system-level simulation environment, to perform both interactive "what if" design exploration as well as more detailed investigations of higher order effects by simply changing the simulation parameters (e.g., optical mesh size, number of mechanical nodes, number of regions of operation for non-linear elements, and minimum time-step) without recourse to lower level simulation tools.

Table 1: Grating Light Valve System Simulation Time

	Mesh	128x128			512x512		
Segments		Mech	Optical	System	Mech	Optical	System
5		0.14	1.99	3.33	0.16	40.79	42.37
11		2.02	2.02	5.30	2.02	41.01	44.49
21		15.60	1.98	19.19	15.43	40.78	58.19
41		119.94	1.99	128.81	124.40	40.33	167.68

3 SUMMARY AND CONCLUSIONS

With this example, we have introduced the challenges in modeling mixed-signal multi-domain microsystems as well as the potentiality of our multi-domain methodology. While we have shown the success of our techniques for a limited number of domains, there is still much work to be done in order to provide a more general multi-domain modeling and simulation environment for mixed domain systems.

REFERENCES

[1]. D. L. Karnoop, and R. C. Rosenberg, System dynamics: a unified approach, John Wiley & Sons Inc., 1975.

[2]. S. P. Levitan, et. al, "System Simulation of Mixed-Signal Multi-Domain Microsystems with Piecewise Linear Models," to be published in IEEE Transactions on CAD of Integrated Circuits and Systems, February, 2003.

[3]. Bloom, D.M., "The Grating Light Valve: Revolutionizing Display Technology," in Proc. of Photonics West, Projection Displays III, 1997.

[4]. T.P. Kurzweg, et. al, "A Fast Optical Propagation Technique for Modeling Micro-Optical Systems," DAC'02, New Orleans, LA, June 10-14, 2002.

[2] For a dual Pentium 1.7 GHz/Xeon processor with 4 GB RAM